DOI 10.5162/16dss2022/P48

Design of an AI-supported Sensor for Process Relevant Parameters in Emulsification Processes

Inga Burke[1], Ahmed S. Youssef[1], and Norbert Kockmann[1]

[1]TU Dortmund University, Department of Biochemical and Chemical Engineering, Laboratory of Equipment Design, Dortmund/Germany
Contact: inga.burke@tu-dortmund.de

Introduction

The development of smart sensors for online process supervision is an increasing trend in the process industry [1]. In particular, multiphase processes benefit from smart image sensors during processing steps such as emulsification. Emulsions consist of two immiscible liquids dispersed in fine droplets and can be found in a variety of daily life and industrial products such as food products, cosmetics, and pharmaceutical productions [2].
Since the droplet size represents a significant parameter determining the progress of the emulsification process and needs to be monitored, an optical sensor is developed for the investigation of the droplet size within the emulsification process. The actual state of the emulsification process is often determined by analog sampling and testing, which results in inefficient process control due to the delay and bias caused by the offline analysis. The use of a smart optical sensor for just-in-time evaluation of the emulsification progress is presented to increase the efficiency of the process and to reduce process costs. In this work, a Deep Learning (DL) approach is applied to digital images for contour recognition that automatically determines the droplet size distribution (DSD) within the emulsification process. For this purpose, the DL algorithm YOLOv4 is used as object detector.

Material and Methods

Experimental Setup

The schematic setup of the emulsification process used in this work is shown in Fig.1. The emulsification process is performed in a glass vessel. The emulsion vessel has a volume of 1L and is temperature-controlled. The temperature control of the emulsion vessel is achieved by a Pilot ONE ministat 230 (Huber Kältemaschinenbau AG, Germany). The production of the emulsion bases on mechanical dispersion by a rotor-stator system. The disperser used (HG-15D, witeg Labortechnik GmBH, Germany) is equipped with a dispersing tool (HT1018, witeg Labortechnik GmBH, Germany), whose rotor has a diameter of 20 mm and stator of 25 mm, resulting in a gap width of 0.35 mm. The emulsion vessel contains four GL-14 fluid connections. Two of these connections are located at the head of the container for sensors to be inserted into the system, e.g. for temperature measurement and control. The two other outlets are located at the lower end of the vessel and on the opposite upper end. These are the connections for a mini channel bypass, in which the optical analysis of the emulsification process takes place. The analytical bypass consists of an FEP tube with an inner diameter of 1.6 mm. The optical analysis includes the optical, non-invasive measurement flow cell made of glass adapted from [3], a microscope (Bresser Science ADL 601P, Bresser GmbH, Germany), and a camera (Z6, Nikon GmbH, Japan) attached to the microscope.

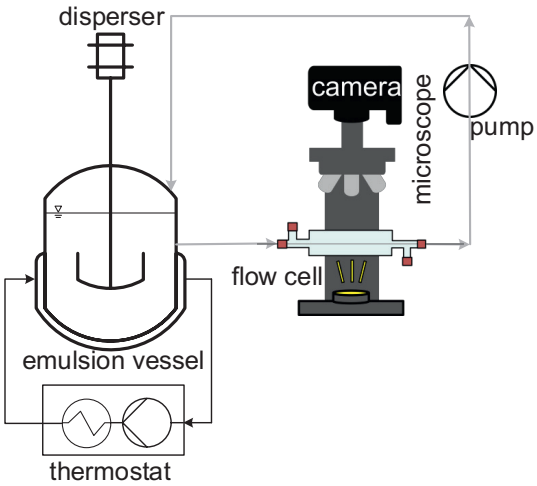

Fig. 1: Schematic experimental setup of the emulsification process with the analytical bypass.

Fig. 2 shows a more detailed image of the optical analysis unit. The measuring cell is shown with the bypass FEP tube, placed under the microscope. For the optical observation of the emulsification process, the flow cell is filled with water to optically compensate the rounding of the tube. Due to the similar refractive index of water (1.3312 - 1.3372) [4] and FEP (1.3380 - 1.334) [5] a distortion-free observation of a water-based emulsion is carried out. Several further investigations confirm this experience [3, 6, 7]. A peristaltic pump (LabDos Easy-Load, HiTec Zang GmbH, Germany) pumps the emulsion through the analytic bypass, where it returns to the emulsion vessel. The volume of the bypass is significantly smaller than the volume of the vessel.

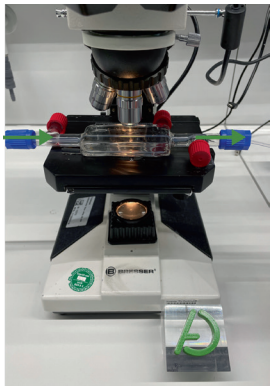

Fig. 2: Setup of the measurement flow cell for optical accessibility of the emulsification process.

Dispersion Experiments

The experiments to generate the training of the DL algorithm, its validation, and the test data set have been carried out in the setup described above. For this purpose, commercially available sunflower oil was dispersed in deionized water as continuous phase. The droplet formation occurs because of high shear rates in the gap between the rotor and stator. The emulsion preparation was done to record initial data sets for the DL algorithm, so the focus is not considered on process parameter settings. The basic parameters of the data set generating experiments are displayed in Tab. 1.

Tab. 1: Process parameter settings.

Process parameter / Operation	Setting
continuous phase	99 vol.-%
disperse phase	1 vol.-%
disperser speed	5000 rpm
temperature in the emulsion vessel	22 °C
flow rate of the analytic bypass	4.225 mL min^{-1}

In the experiments, the continuous phase and dispersed phase were fed into the emulsion vessel, where the emulsification process takes place. The emulsion is pumped through the analysis bypass to achieve optical accessibility and to capture the process progress. Therefore, the process was observed over the whole process time for data collection using the optical sensor.
The optical sensor in form of a camera (Nikon Z6) observes the progress of the emulsification experiments via a bypass and detects the DSD of the occurring droplets. The set magnification of the microscope, to which the optical sensor is attached, is 10x. Depending on the used quality of the image capturing, the optical information is converted to a pixel-to-µm ratio to add a scale bar that is used for the droplet size analysis.

Dataset Construction

The dataset, which is used to train the DL algorithm YOLOv4, was recorded based on the experiments described in the previous section on dispersion experiments. Tab. 2 shows the subdivision of the data set into parts for training, validation, and testing. A second data set was recorded and labeled to test the algorithm in order to verify the robustness of the applied methodology. The second data set was recorded using a different light source, which results in a different color temperature of the captured images. The data set for extended testing of YOLOv4 is defined in Tab. 2, too.

Tab. 2: Data set split.

Aspect	Training	Validation	Test 1	Test 2
No. images	32	8	7	10
No. objects	7075	1769	978	2040

The training and validation data sets share common characteristics as having been divided in a ratio of 80:20. Images taken for the different test sets are given in Fig. 3.

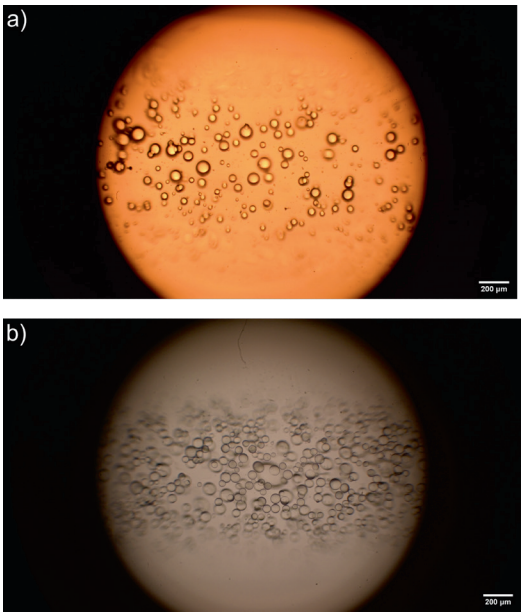

Fig. 3: Example image for a) test data set 1, and b) test data set 2.

YOLOv4 was trained to detect two different classes, the class “droplet” and “outRange”. Since droplets that are out of focus (or out of range) are not usable for an accurate representation of the droplet size, the class “outRange” is introduced to minimize resulting errors of droplets that appear smaller or even bigger because there are not focused.

Optical Sensor – Neural Network Implementation

Since smart process control is an increasing trend in the process industry, a digital camera is used as an optical sensor for the investigation of droplet sizes within an emulsification process. To obtain the droplet size the AI-based object detection YOLOv4 is used.

YOLOv4 is capable of detecting objects and assigning a confidence score to this object in a single evaluation. It combines a series of different computer vision techniques to achieve efficiently real-time object detection. YOLOv4 predicts the class of the detected object, the probability of the class as well as the position of the object within the image. By drawing bounding boxes around the detected classes YOLOv4 gives information about the center position of the bounding box (b_x, b_y), the width b_w, and the height b_h of the box as well as about the class of the detected object *c*.[8] Fig. 4 shows the overall workflow for droplet detection and size determination. An image series of the emulsification process captured by the digital camera is used as the input for the AI-based examination. The used object detection method, feature extraction, and processing of the output run in a closed processing unit. The computer-processing unit (CPU) is an *Intel Xeon* with 3.3 GHz, ten cores, and 128 GB of RAM. The graphical-processing unit (GPU) is an *NVIDIA* Quadro RTX 5000 with 16 GB and 3072 CUDA parallel-processing cores.

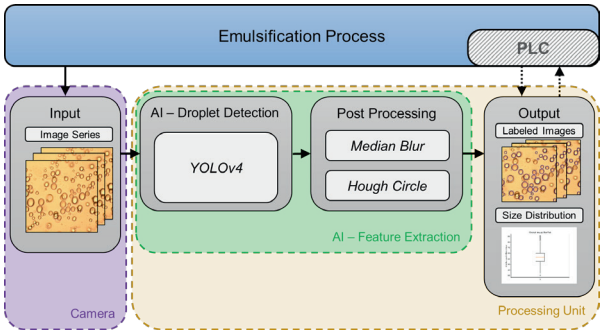

Fig. 4: Flow sheet of the developed workflow with YOLOv4 as network including future PLC connection.

During droplet detection, the input images, which show the emulsification process, are examined. The detected droplets of the class "droplet" are finally evaluated. The bounding boxes detected by YOLOv4 contain the identified focused droplets. The determination of the individual droplet sizes is necessary to determine a droplet size distribution characterizing the process progress. Each bounding box of the class "droplet" is examined individually using the feature detection method *Hough Circle* [9]. *Hough Circle* detects circles in a grayscale image. For this purpose, the center of the detected circle [a,b] as well as the radius R are part of the output [a, b, R].[10] Before applying *Hough Circle*, the median blur filter is applied to get rid of noises within the image of the detected bounding box. These features of each detected bounding box of the class "droplet" are extracted to infer the individual droplet sizes. In the present case, the size of the droplet is unknown, thus multiple circles with different radii are drawn, and the point that has the highest number of intersections is considered the center of the required circle. The radius is the radius of the circles that intersect in the center of the main circle, as shown in Fig. 5. Due to the directional manipulation of the *Hough Circle* descriptive parameters in OpenCV [9], the accuracy of detecting the droplets inside the bounding boxes is increased. An increase in accuracy significantly influences the credibility of the statistical evaluation of the emulsion process.

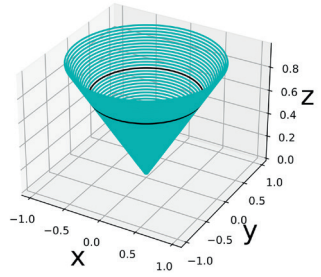

Fig. 5: *Hough Circle* transformation examples: 3D drawing of circle detection with unknown radius.

Since the output of *Hough Circle* is the radius of the detected droplets, the calculation of the droplet diameter is possible. By evaluating at least 600 droplets out of at least ten different process-describing images, a statistical evaluation is performed. A boxplot of the results is printed as the result of the statistical evaluation.

The entire YOLOv4 implementation for training, validation, and testing is based on a *darknet* backend. *Darknet* is an open-source framework for convolutional neural networks (CNN). It can be used with CPU and GPU.[11] The final detection is implemented using OpenCV as open source library. The programming language is Python (Version: 3.8.13, Delaware, USA).

Comparing Image Analysis

A comparative image analysis methodology is used to assess the trustworthiness of the resulting droplet size distributions and, thus, to evaluate the optical sensor. For this purpose, an independent evaluation of the images considered by YOLOv4 is performed manually in ImageJ [12]. In addition, only the class "droplet" was considered for the evaluation. Assuming that the droplets are spherical, the area of the droplets was used to determine the droplet diameter.

Evaluation Criterions

To get quantitative information of the performance of the neural network and about how well YOLOv4 detects and recognizes classified objects in this case, precision and recall are typically applied metrics [13]. The recall R and precision P of a model are defined by their true positives tp, false positives fp, and false negatives fn.

$$R = \frac{tp}{tp + fn} \quad (1)$$

$$P = \frac{tp}{tp + fp} \quad (2)$$

Additionally, the mean average precision (mAP) is used to evaluate the training of the neural network. The mAP is calculated by the mean of the average precision (AP) across all classes. AP is defined as the area under the curve of R and P.[14]

Results and Discussion

During training, the neural net's accuracy increases after 6000 iterations of training, where the neural net reaches an mAP of 80.65 % for an overall training time of 7:06 h and an Intersection of Union threshold (IoU) of 0.50. Intersection over Union indicates the overlap of the predicted bounding box coordinates to the ground truth box. Even for longer training duration, no better results were achieved. The average precision of the class "droplet" is 85.19 %, which indicates a successful detection of this class. Obtained on the previously unseen first test data set, the final mAP (min. IoU 0.5) and the AP for the class "droplet" are 76.09 % and 85.80 %, respectively. This results in 129 out of 978 total objects being misclassified as "droplets" or failing to achieve an IoU of 0.5 for a confidence score of 0.8 (fp). This results in R= 0.52, which means that 52.00 % of the predictions are actually predicted. Although the recall can be improved, there is no big influence on the statistical evaluation of the emulsification process, since the droplet size distribution is calculated from at least ten different images. A high precision that the detected object is a "droplet" is therefore more important than detecting every single object. Finally, it is more important to have a higher precision in detection, since it indicates how much the model is reliable. Since the precision of the model is P= 0.75 for a confidence score of 0.8, trustworthiness is given. The mAP clearly articulates the tradeoff of using precision and recall as independent metrics. Having a high precision, but low recall results in having an accurate model when classifying a positive object but it may classify only some of the positive samples. The mAP of 76.09 % leads to 505 tp, 170 fp, and 473 fn detected. This means that 505 objects out of 978 are detected correctly, wheter 170 being misclassified as "droplets" or failed to achieve an IoU of 0.5 for a confidence score of 0.8, and 473 being not classified at all or failed to achieve the IoU of 0.5.

However, since YOLOv4 misclassifies some objects, the trustworthiness of the final droplet size distributions is evaluated. Additionally, the impact of the "outRange" depends on the setup of the optical accessibility as well as on the content of the dispersed phase. Since there are many overlapping droplets in the measurement flow cell, there is no chance to evaluate droplets in the background of the image.

Comparing Image Analysis

It is important for process decisions to know whether the object detection is right or wrong. For this reason, the trustworthiness of the results as well as the impact of incorrectly detected droplets used for the evaluation need to be considered. To investigate both, a comparison with another, manually performed, image-based evaluation is carried out.

Fig. 6 shows the resulting boxplot of the evaluation of the same images of the emulsification process.

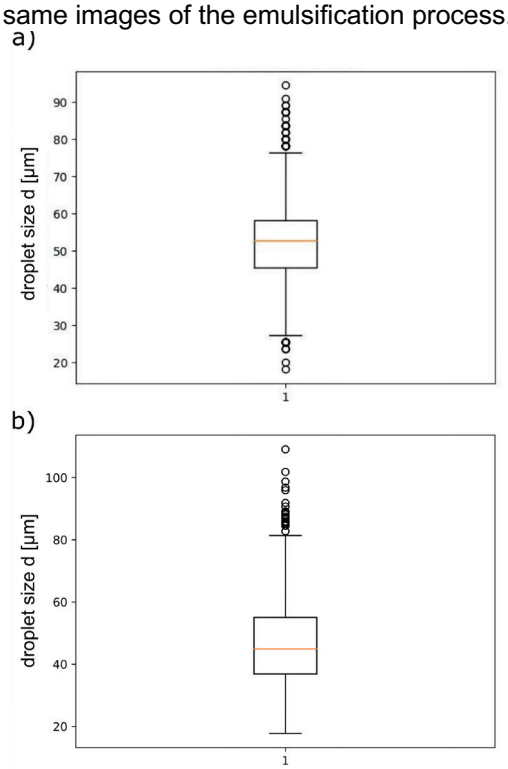

Fig. 6: Resulting boxplot for image evaluation of emulsification process by using a) AI and feature extraction, and b) manual evaluation in ImageJ.

The droplet detection and droplet size analysis were done with a set confidence score of 0.9 concerning the droplet class. A confidence score of 90 % means that the algorithm is 90 % sure that the detected object belongs to the class "droplet". The used DL algorithm YOLOv4 as well as the manual evaluation in ImageJ were applied to 15 images with a total amount of 1225 detected droplets using YOLOv4. The overall detection and evaluation time for these images is 7.7 seconds. The detected focused droplets using ImageJ in these 15 images were in total 924. This difference in the number of evaluated droplets occurs because of the decision on which droplet is in range and which one is out of range. This decision depends on the person, who did the labeling and the ImageJ comparison, and due to the number of droplets, that are falsely detected by YOLOv4.

By comparing the median droplet size ($d_{50,ImageJ}$ = 44.92 µm, $d_{50,AI}$= 52.73 µm) there is a difference of 7.81 µm. The values of the first and third quartile are

also varying, but the interquartile range (IQR), the difference between the third and first quartile, is similar (IQR_{ImageJ}= 18.19 µm to IQR_{AI}= 12.73 µm). However, the mean and the IQR of the distribution are in similar ranges.

The evaluated droplet size range in a) and b) are close to each other, which means that the results from the droplet detection and subsequent size determination are reliable. Deviations can be explained on the one hand by the fact that for the manual evaluation the circular area was assumed as the basis for calculation, but also by the incorrect evaluation of non-focused droplets in both evaluation cases. The work shows that AI-based droplet detection provides similar DSD compared to manual evaluation while requiring only a fraction of the time to evaluate (7.7 s in total). This enables future online monitoring of DSD, since droplets can be successfully detected, and plausible size determination can be performed. Further investigation, what method (manual vs. AI) is more trustworthy needs to be performed by using a reference with known size distribution.

Robustness

To demonstrate the model's flexibility and robustness, an additional test with a second, unseen image set is carried out. The images of the emulsification process were taken with different illumination source resulting in a different color temperature. No additional training was performed for this testing. The final mAP at 0.50 IoU is 82.81 %, so 6.72 % higher than for the first test data set. This leads into a more reliable tradeoff of precision and recall. The AP for the class "droplets" is 88.64 %, which is again an increase in comparison to the first data set. The sensitivity to predict the true positive is R= 0.49, and the precision is P= 0.81. This leads to 120 droplets out of 2040 total objects that were misclassified or failed to achieve the 0.5 IoU, for a confidence score of 0.8. Since there is an increase in the precision and just a slight decrease in the recall, the overall detection quality of "droplets" increased for this different light setting. In conclusion, these results show the flexibility and robustness of the used algorithm regarding changes in the experimental setup. Further investigation of using this lighting source in the experimental setup and including an additional training data set out of these data are planned.

Conclusions and Outlook

In summary, a workflow to design a smart sensor for emulsification analysis in form of a digital camera was shown. The used object detector, YOLOv4 as chosen DL algorithm, was trained, and used for object detection, and an additional feature extraction step, using *Hough Circle*, was added to analyze the droplet sizes. The work demonstrates that YOLOv4 can be used to identify droplets in an emulsification process. The trustworthiness and robustness of the used algorithm were discussed, with the result that a deeper investigation regarding the correct size determination is needed since the used pixel-to-µm ratio is not working for droplets, which are out of focus. A comparison with a manual image evaluation also demonstrates that the AI-based result has a similar DSD. In addition to saving time, one advantage of AI-based droplet detection is that the deviation of detection by the algorithm is constant, which is not necessarily the case with manual evaluation, as this depends on the user. Further investigations are essential in order to evaluate the classification and the influence of the "outRange" class more precisely. In addition, an applicability to emulsions with higher disperse phase fractions is required.

The AI-supported sensor is used to determine quantitative parameters such as mean droplet size based on image data. The next step is the use of data-driven modeling, which aims to develop a real-time determination of process-relevant parameters. This can be used to control a stable and efficient emulsification process. For this aim, a programmable logic control will be implemented to communicate with the actuators and sensors of the setup in order to control the emulsification process more efficiently, as already shown in Fig. 4.

References

[1] KOCKMANN, N.; BITTORF, L.; KRIEGER, W.; REICHMANN, F.; SCHMALENBERG, M.; SOBOLL, S.: Smart Equipment – A Perspective Paper. *Chem. Ing. Technik* 90 (2018), no. 11, pp 1806-1822, doi.org/10.1002/cite.201800020.

[2] HIEMENZ, P.; RAJAGOPALAN, R. (editor): Principles of Colloid and Surface Chemistry, Revised and Expanded, Crc Press Inc, 3rd edition, 1997.

[3] SCHMALENBERG, M.; SALLAMON, F.; HAAS, C.; KOCKMANN, N.: Temperature-Controlled Minichannel Flow-Cell for Non-Invasive Particle Measurements in Solid-Liquid Flow. *Proceeding of ASME 2020 18th International Conference on Nanochannels, Microchannels, and Minichannels* (2020), V001T16A005. ASME, https://doi.org/10.1115/ICNMM2020-1062.

[4] BUDWIG, R.: Refractive index matching methods for liquid flow investigations. *Experiments in Fluids* (1994), pp. 350–355.

[5] WYPYCH, G.: Handbook of Polymers: FEP fluorinated ethylene-propylene copolymer, 2016.

[6] SCHMALENBERG, M.; KREIS, S.; WEICK, L.K.; HAAS, C.; SALLAMON, F.; KOCKMANN, N.: Continuous Cooling Crystallization in a Coiled Flow Inverter Crystallizer Technology – Design, Characterization, and Hurdles. *Processes* 9 (2021), p.1537, https://doi.org/10.3390/pr9091537.

[7] KRIEGER, W.; HÖRBELT, M.; SCHUSTER, S.; HENNEKES, J.; KOCKMANN, N.: Kinetic Study of Leuco-Indigo Carmine Oxidation and Investigation of Taylor and Dean Flow Superposition in a Coiled Flow

Inverter. *Chem. Eng. Technol*. 42 (2019), 10, pp. 2052–2060, https://doi.org/10.1002/ceat.201800753.

[8] BOCHKOVSKIY A., WANG, C.-Y.; LIAO H.-Y- M.: YOLOv4: Optimal Speed and Accuracy of Object Detection. (2020), https://doi.org/10.48550/arXiv.2004.10934.

[9] OpenCV Hough Circle Documentation, https://docs.opencv.org/3.4/d4/d70/tutorial_hough_circle.html; (last access: 2022-10-17).

[10] FERGUSON, T.; BAKER, D.: Feature Extraction Using the Hough Transform, *Computer Science* (2002).

[11] SOWA, P.; IZYDORCZYK, J.: Darknet on OpenCL: A multiplatform tool for object detection and classification. *Concurrency Computat. Pract. Exper*. 34 (2022), https://doi.org/10.1002/cpe.6936.

[12] SCHNEIDER, C.A.; RASBAND, W.S.; ELICEIRI, K.W.: NIH Image to ImageJ: 25 years of image analysis. *Nature Methods* 9 (2012), 7, pp. 671-675, doi:10.1038/nmeth.2089.

[13] KOSSMANN, D.; WILHELM, T.; FINK, G. A.: Towards Tackling Multi-Label Imbalances in Remote Sensing Imagery. *25th International Conference on Pattern Recognition (ICPR)*; IEEE (2021); pp.5782−5789.

[14] HEMANTH,D.J.; ESTRELA. V.V.: Deep Learning for Image Processing Applications. *Advances in Parallel Computing* (2017). IOS Press.

Acknowledgments

The authors thank Carsten Schrömges for his support and the German Federal Ministry for Economic Affairs and Climate Action (BMWK) for funding this research as part of AiF (Support code: KK5168501).